Impact of convective boundary condition on MHD flow through a porous medium on a vertical plate in the presence of heat generation/absorption, using Galerkin Weighted Residual Method on Wolfram Mathematica

By

Akinbo, Bayo Johnson (Ph.D)

Akaje, Toyin Wasiu (Ph.D)

Federal College of Education,

Abeokuta,

Ogun State, Nigeria

INTRODUCTION

The case of heat and mass transfer in both **Newtonian and non-Newtonian types of fluid** have great importances in industries as well as science and engineering fields, particularly in this technology-driven world among which are polymer sheet, glass-fabric, biological fluid, application of paint and petroleum production, etc. On the account of various applications of the heat transfer phenomenon, a good number of researchers have contributed to the literature.

- Makinde [1-4]
- Hayat et al. [5-7]
- Akinbo and Olajuwon [8-12]
- Akaje and Olajuwon [13-17]

Motivated by the applications and previous workdone by different authors, this particular work intends to investigate the behaviors of heat generation/absorption on Magnetohydrodynamics (MHD) flow over a vertical plate with convective boundary condition. The study is considered with a medium porosity which is exposed a magnetic intensity

2. Mathematical Formulation

We consider a steady laminar two-dimensional boundary layer flow of a stream of cold incompressible electrically conducting fluid along a vertical plate embedded in porous medium at temperature T_∞ which takes place in the presence of heat source and chemical reaction. The left surface of the plate is assumed to be heated by convection from a hot fluid at temperature T_f that produces a heat transfer coefficient h_f . The cold fluid in contact with the upper surface of the plate generate heat internally at volumetric rate Q_0. A magnetic field B_0 of uniform strength is applied transversely to the direction of the flow while the magnetic Reynolds number is assumed to be small, therefore, the induced magnetic field is not taken into account and the joule heating in energy equation is assumed to be neglected as it really very small in slow motion free convection flow. $x-axis$ is taken parallel to the plate direction and $y-axis$ normal to it. C_w is the concentration at the surface of the plate while T_∞ and C_∞ denote ambient temperature and concentration respectively. The fluid temperature and concentration are respectively taken as T and C while the fluid velocity in x and y dircetions are respectively denoted by u and v.

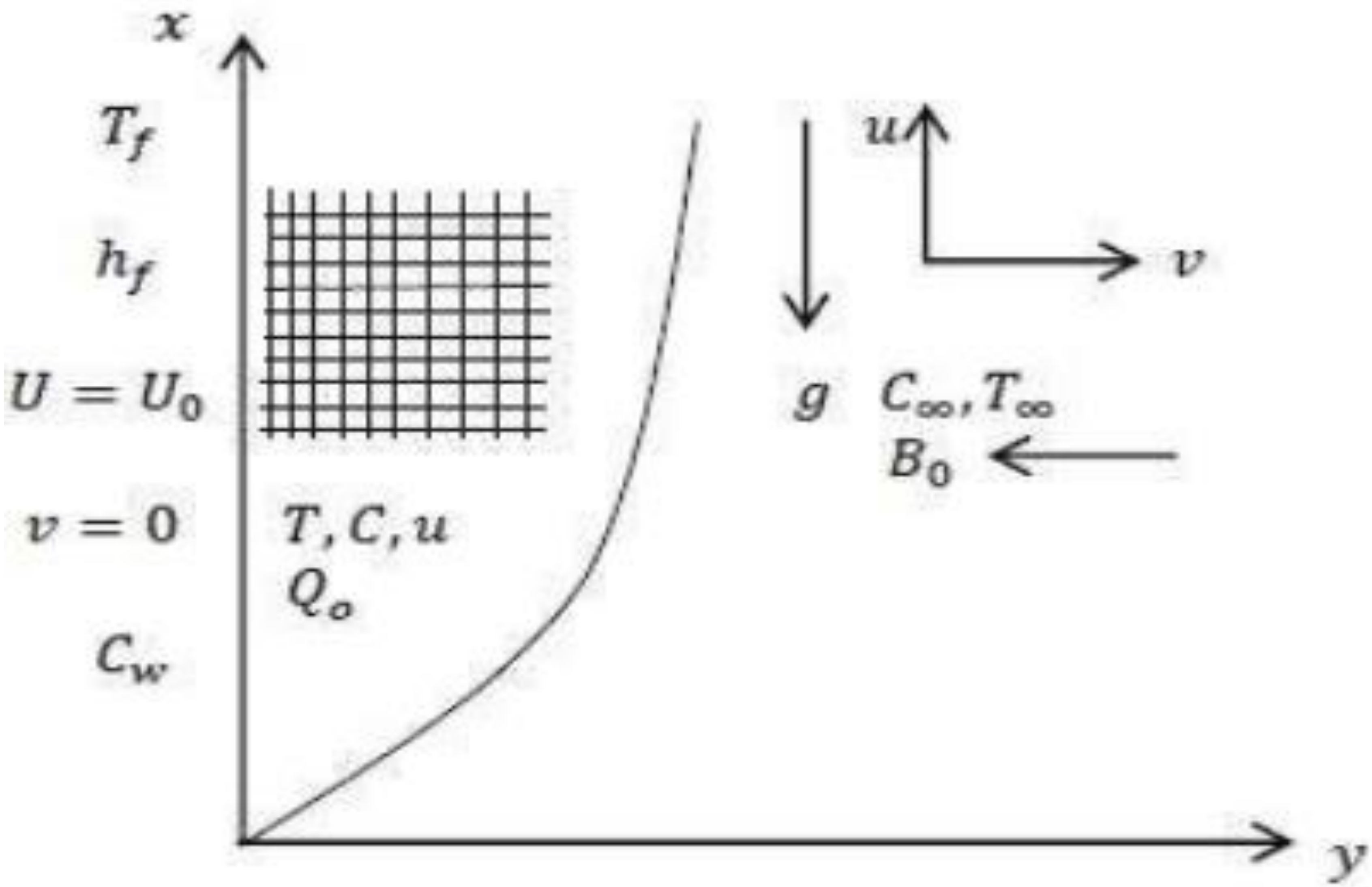

Figure 1 Flow configuration and coordinate system.

Subject to the assumption stated above and usual Boussinesq's approximation, the governing equations of this present problem can be expressed as

$$\frac{\partial u}{\partial x}+\frac{\partial v}{\partial y}=0 \tag{1}$$

$$u\frac{\partial u}{\partial x}+v\frac{\partial u}{\partial y}=\mathrm{v}\frac{\partial^2 u}{\partial y^2}-\frac{\sigma B_0 u}{\rho}-\frac{\mathrm{v}}{K}u+g\,\beta_T(T-T_\infty)+g\,\beta_c(C-C_\infty) \tag{2}$$

$$u\frac{\partial T}{\partial x}+v\frac{\partial T}{\partial y}=\alpha\frac{\partial^2 T}{\partial y^2}+\frac{\mathrm{v}}{C_p}\left(\frac{\partial u}{\partial y}\right)^2-\frac{1}{\rho C_p}\frac{\partial q_r}{\partial y}+\frac{Q_0(T-T_\infty)}{\rho C_p} \tag{3}$$

$$u\frac{\partial C}{\partial x}+v\frac{\partial C}{\partial y}=D\frac{\partial^2 C}{\partial y^2} \tag{4}$$

Where D denotes mass diffusivity, α body forth thermal diffusivity, g represents acceleration which occur as a result of gravity, ρ typifies density, σ shows electrical conductivity, β_T and β_c respectively connotes thermal and concentration expansion coefficient, Q_0 is the volumemetric heat generation/absorption coefficient, C_p denotes specific heat at constant pressure while v is the kinematics viscosity, (u,v) are the components of velocity at any point (x,y). Concur with the following conditions

$$U(x,0)=\ U_0,\ V(x,0)=0,\ -k\frac{\partial T(x,0)}{\partial y}=h_f[T_f-T(x,0)],\ C_w(x,0)=Ax^\lambda+C_\infty$$

$$U(x,\infty)=0,\ T(x,\infty)=T_\infty,\ \ C(x,\infty)=C_\infty \tag{5}$$

Here, λ connotes the index power of the concentration and k thermal conductivity coefficient. The radiative heat flux by Roseland was adopted and expressed as

$$q_r = \frac{-4\sigma^*}{3K^*}\frac{\partial T^4}{\partial y} \tag{6}$$

Where K^* stands as coefficient of mean of absorption and σ^* typifies Sterfan-Boltzmann constant. Bearing in mind that the temperature differences within the flow are such that equation (6) can be linearized subjecting T^4 into Taylor series around T_∞ and disuse higher-order terms gives

$$T^4 \approx 4T_\infty^3 T - 3T_\infty^4 \tag{7}$$

By the introduction of Eq. (6) and (7) in Eq. (3), we have

$$u\frac{\partial T}{\partial x} + v\frac{\partial T}{\partial y} = \alpha\frac{\partial^2 T}{\partial y^2} + \frac{\mathrm{v}}{C_p}\left(\frac{\partial u}{\partial y}\right)^2 + \frac{16\sigma T_\infty}{3K^*\rho C_p}\frac{\partial^2 T}{\partial y^2} + \frac{Q_0(T - T_\infty)}{\rho C_p} \tag{8}$$

Following Makinde [1], Eq. (1) is trivially satisfied through the stream function expressed by

$$u = \frac{\partial \psi}{\partial y} \quad and \quad v = -\frac{\partial \psi}{\partial x} \tag{9}$$

Invoking

$$\eta = y\sqrt{\frac{U_0}{\mathrm{v}x}}\ , \qquad \psi = \sqrt{\mathrm{v}xU_0}f(\eta), \tag{10}$$

where U_0 connotes the velocity of the plate and,

$$\theta(\eta) = \frac{T - T_\infty}{T_f - T_\infty}, \qquad \emptyset(\eta) = \frac{C - C_\infty}{C_w - C_\infty} \tag{11}$$

Body-forth non-dimensional; temperature and concentration. Applying equations (9-11) into Eqs (1)-(2), (4)-(5) and modified equation (8), we have

$$\frac{d^3 f(\eta)}{d\eta^3} + \frac{1}{2}f(\eta)\frac{d^2 f(\eta)}{d\eta^2} - (Ha + P_s)\frac{df(\eta)}{d\eta} + Gr\theta(\eta) + Gc\emptyset(\eta) = 0 \tag{12}$$

$$\left(1 + \frac{4}{3Ra}\right)\frac{d^2\theta(\eta)}{d\eta^2} + PrEc\left(\frac{d^2 f(\eta)}{d\eta^2}\right)^2 + \frac{1}{2}Prf(\eta)\frac{d\theta(\eta)}{d\eta} + Q\theta(\eta) = 0 \tag{13}$$

$$\frac{d^2\emptyset(\eta)}{d\eta^2} + \frac{1}{2}Scf(\eta)\frac{d\emptyset(\eta)}{\partial\eta} = 0 \tag{14}$$

Where the derivatives are considered with respect to η and

$$Ha = \frac{\sigma B_0^2 x}{\rho U_0}, Gr = \frac{g\beta_T\left(T_f - T_\infty\right)x}{U_0^2}, Gc = \frac{g\beta_c(C_w - C_\infty)x}{U_0^2}, Bi = \frac{hf}{k}\sqrt{\frac{\text{v}x}{U_0}}, \alpha = \frac{k^*}{\rho C_\rho}$$

$$P_s = \frac{\text{v}x}{KU_0}, Pr = \frac{\text{v}}{\alpha}, Sc = \frac{\text{v}}{D}, Q = \frac{xQ_0\text{v}}{KU_0}, Ec = \frac{U_0^2}{C_p\left(T_f - T_\infty\right)}, Ra = \frac{4\sigma T_\infty}{KK^*}, \alpha = \frac{k^*}{\rho C_p} \quad (15)$$

where Ha represents local magnetic parameter, (Gr, Gc) shows local thermal and solutal Grashof number respectively, Bi stands for Boit number , Pr portrays Prandtl number, Sc body–forth Schmidt number, P_s connotes Porosity parameter, Q denotes heat generation parameter, Ec stands for Eckert number while Ra typifies Radiation parameter. Agreed with the following boundary conditions

$$f(0) = 0, \; f^{'}(0) = 1, \; \theta^{'}(0) = Bi[\theta(0) - 1], \; \emptyset(0) = 1 \quad (16)$$

$$f^{'}(\infty) = 0, \; \theta(\infty) = 0, \; \emptyset(\infty) = 0 \quad (17)$$

Following Lakshmi et'al. [19]. Keeping in mind that the local parameters Bi, Ha, Gr, Gc, Q and P_s in (12-14) are functions of x. We obtained the similarity solution by holding on the following parameters

$$h_f = \frac{a}{\sqrt{x}}, \qquad \sigma = \frac{b}{x}, \qquad \beta_T = \frac{c}{x}, \qquad \beta_c = \frac{d}{x}, \qquad Q_0 = \frac{e}{x}, K = \frac{x}{q} \quad (18)$$

Where $a, b, c, d\ e$ and q are constants taken with right dimension.

3.0 Method of Solution

Non-linear differential equations are practically crucial in mathematical modeling. They can be tackled via different methods, such as; Adomian Decomposition, Homotopy perturbation and so on. Galerkin Weighted Residual Method (GWRM) is chosen over others due to its efficiency to provide accurate results while dealing with the coupled higher-order differential equations. In agreement with Akinbo and Olajuwon [20], from equation (12)-(14) and (16)-(17), we assumed the trial functions

$$f = \sum_{i=0}^{12} a_i e^{-\frac{i\eta}{4}} \; , \theta = \sum_{i=1}^{13} b_i e^{-\frac{i\eta}{4}} \; , \qquad \emptyset = \sum_{i=1}^{13} c_i e^{-\frac{i\eta}{4}} \tag{21}$$

Imposing the boundary conditions (15), we have

$$a_0 + a_1 + a_2 + a_3 + a_4 + a_5 + a_6 + a_7 + a_8 + a_9 + a_{10} + a_{11} + a_{12} = 0 \tag{22}$$

$$b_1 + b_2 + b_3 + b_4 + b_5 + b_6 + b_7 + b_8 + b_9 + b_{10} + b_{11} + b_{12} + b_{13} - 1 = 0 \tag{23}$$

$$c_1 + c_2 + c_3 + c_4 + c_5 + c_6 + c_7 + c_8 + c_9 + c_{10} + c_{11} + c_{12} + c_{13} - 1 = 0 \tag{24}$$

and for $f'(0)=1,\ \theta'(0)=Bi[\theta(0)-1]$, we have

$$-\frac{1}{4}a_1-\frac{1}{2}a_2-\frac{3}{4}a_3-a_4-\frac{5}{4}a_5-\frac{3}{2}a_6-\frac{7}{4}a_7-2a_8-\frac{9}{4}a_9-\frac{5}{2}a_{10}$$

$$-\frac{11}{4}a_{11}-3a_{12}-1 \tag{25}$$

$$-\left(\frac{1}{4}+Bi\right)b_1-\left(\frac{1}{2}+Bi\right)b_2-\left(\frac{3}{4}+Bi\right)b_3-(1+Bi)b_4-\left(\frac{5}{4}+Bi\right)b_5$$

$$-\left(\frac{3}{2}+Bi\right)b_6-\left(\frac{7}{4}+Bi\right)b_7-(2+Bi)b_8-\left(\frac{9}{4}+Bi\right)b_9-\left(\frac{5}{2}+Bi\right)b_{10}$$

$$-\left(\frac{11}{4}+Bi\right)b_{11}-(3+Bi)b_{12}-\left(\frac{13}{4}+Bi\right)b_{13}+Bi \tag{26}$$

Eq. (17) automatically agreed. In accordance with the rule of the solution, the application of Eq. (21) and Eq. (12-14) give the residual functions R_f, R_θ and $R_\emptyset$ (See Razaq and Aregbesola [20]) which are multiplied by $e^{-\frac{j}{4}\eta}\ \forall\ j\in\mathbb{Z}$, and successfully integrated under the domain. Here, the algebraic equations emanated are tackled with computer MATHEMATICA package and the results obtained are discussed accordingly.

4. Validation of the study

Implementation of numerical computation with the previous workdone was first considered by comparing it with the results with Makinde [21] by setting $P_s = 0,\ Q = 0,\ Ra = 0,\ Ec = 0$. The result are found to be in excellent agreement as displayed in Table 1.

Table 1: The present result with Makinde [21]

						Makinde [21]				**Present result**			
Ha	Gr	Gc	Bi	Pr	Sc	$f''(0)$	$-\theta'(0)$	$\theta(0)$	$-\phi'(0)$	$f''(0)$	$-\theta'(0)$	$\theta(0)$	$-\phi'(0)$
0.1	0.1	0.1	0.1	0.72	0.62	−0.402271	0.078635	0.213643	0.3337425	−0.402270	0.078634	0.213636	0.3337431
1.0	0.1	0.1	0.1	0.72	0.62	−0.352136	0.273153	0.726846	0.3410294	−0.352135	0.273152	0.726839	0.3410288
10	0.1	0.1	0.1	0.72	0.62	−0.329568	0.365258	0.963474	0.3441377	−0.329567	0.365256	0.963473	0.3441369
0.1	0.5	0.1	0.1	0.72	0.62	−0.322212	0.079173	0.208264	0.3451301	−0.322211	0.079172	0.208261	0.3451300
0.1	1.0	0.1	0.1	0.72	0.62	−0.231251	0.079691	0.203088	0.3566654	−0.231250	0.079690	0.203085	0.3566647
0.1	0.1	0.5	0.1	0.72	0.62	−0.026410	0.080711	0.192889	0.3813954	−0.026408	0.080710	0.192887	0.3813960
0.1	0.1	1.0	0.1	0.72	0.62	0.3799184	0.082040	0.179592	0.4176697	0.379917	0.082035	0.179590	0.4176695
0.1	0.1	0.1	1.0	0.72	0.62	−0.985719	0.074174	0.258252	0.2598499	−0.985718	0.074173	0.258251	0.2598501
0.1	0.1	0.1	5.0	0.72	0.62	−2.217928	0.066156	0.338435	0.1806634	−2.217927	0.066154	0.338429	0.1806631
0.1	0.1	0.1	0.1	1.00	0.62	−0.407908	0.081935	0.180640	0.3325180	−0.407907	0.081935	0.180637	0.3325176
0.1	0.1	0.1	0.1	7.10	0.62	−0.421228	0.093348	0.066513	0.3305618	−0.421227	0.093352	0.066512	0.3305617
0.1	0.1	0.1	0.1	0.72	0.78	−0.411704	0.078484	0.215159	0.3844559	−0.411703	0.078482	0.215158	0.3844556

Table2. Significant embedded parameter on Skin-friction, Nusselt number, plate surface temperature and Sherwood number

Ha	Gr	Gc	Bi	Ec	P_s	**Q**	Pr	Sc	Ra	$f''(0)$	$-\theta'(0)$	$\theta(0)$	$-\emptyset'(0)$
0.1	**0.1**	**0.1**	**0.1**	**0.1**	**0.1**	**0.01**	**0.72**	**0.62**	**0.7**	−0.451814	0.059056	0.409439	0.331231
0.5										−0.738708	0.052564	0.474363	0.290705
1.0										−1.004783	0.045898	0.541023	0.256780
	0.5									−0.273902	0.063970	0.360297	0.364958
	1.0									−0.095755	0.066590	0.334104	0.390016
		0.5								−0.098393	0.064039	0.359606	0.375238
		1.0								0.294958	0.066468	0.335323	0.410769
			0.5							−0.405655	0.121882	0.756237	0.341324
			1.0							−0.392376	0.141350	0.858650	0.343997
				1.0						−0.423552	0.041618	0.583823	0.338065
				3.0						−0.374099	0.010851	0.891482	0.348926
					0.5					−0.738708	0.052564	0.474363	0.290705
					1.0					−1.004783	0.045898	0.541023	0.256780
						0.04				−0.434812	0.051004	0.489963	0.336591
						0.07				−0.402381	0.035800	0.641997	0.346015
							1.0			−0.464224	0.064457	0.355435	0.326853
							3.0			−0.489839	0.077351	0.226490	0.318814
								0.24		−0.420466	0.061499	0.385006	0.180222
								0.78		−0.459254	0.058601	0.413994	0.382780
									2.0	−0.470403	0.067197	0.328028	0.324677
									3.0	−0.474379	0.069079	0.309208	0.323346

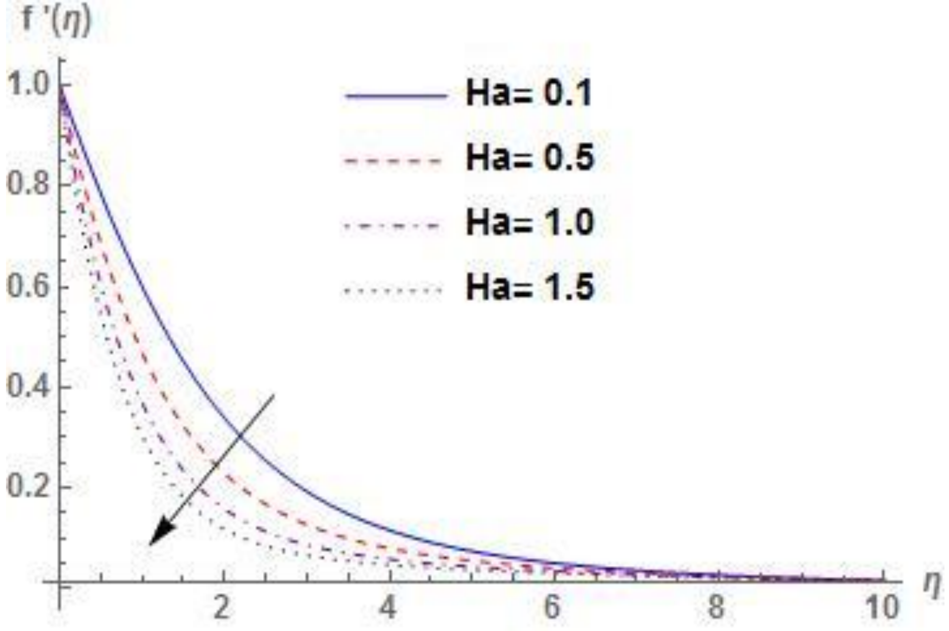

Fig.2 significant of *Ha* on Velocity $f'(\eta)$

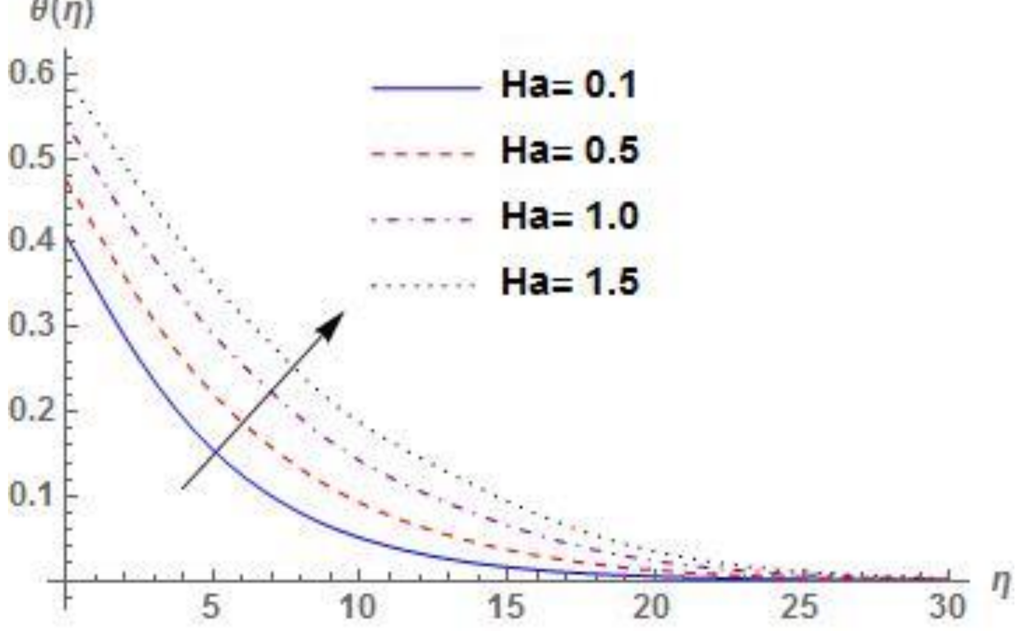

Fig.3 significant of *Ha* on temperature $\theta(\eta)$

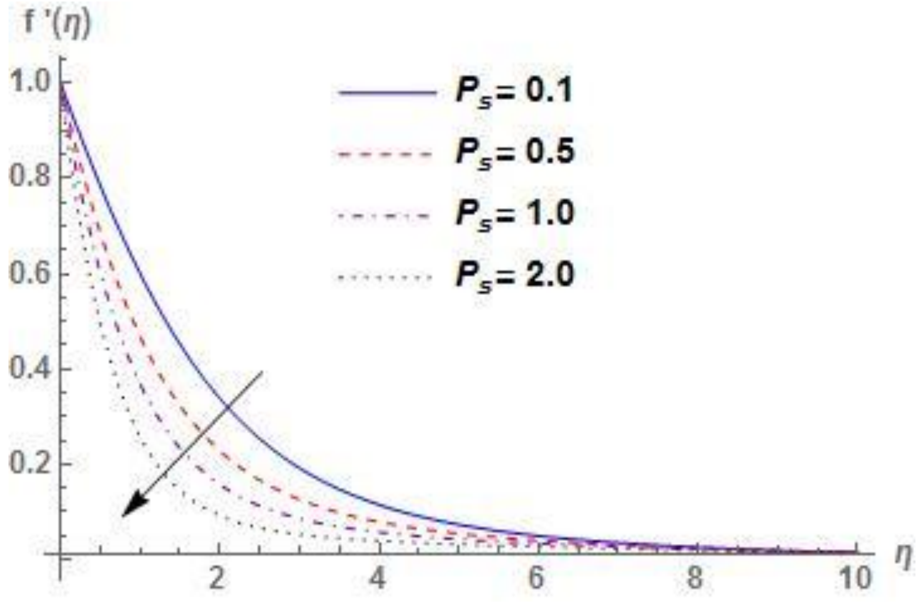

Fig. 4 significant of P_s on Velocity $f'(\eta)$

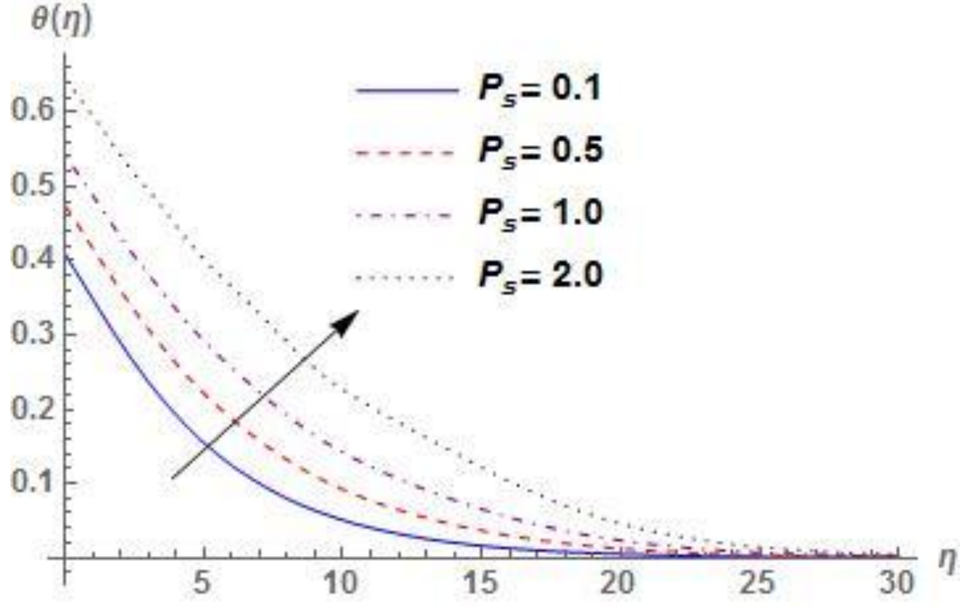

Fig. 5 significant of P_s on temperature $\theta(\eta)$

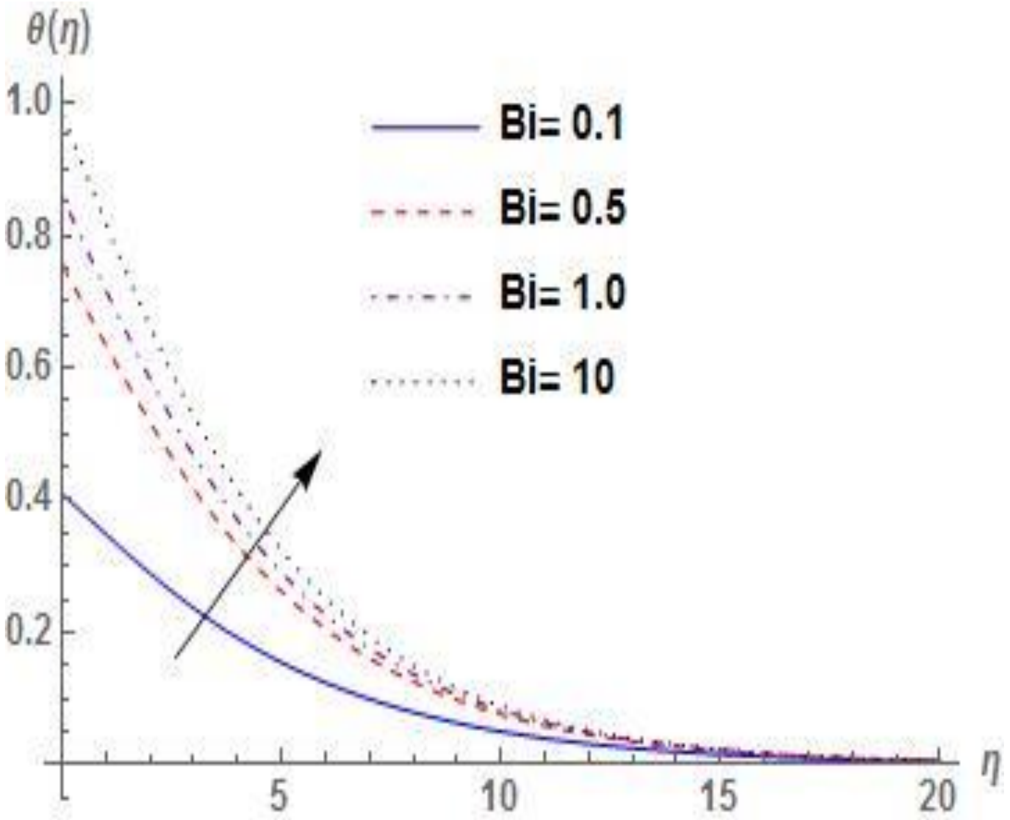

Fig. 6 significant of Bi on Temperature $\theta(\eta)$

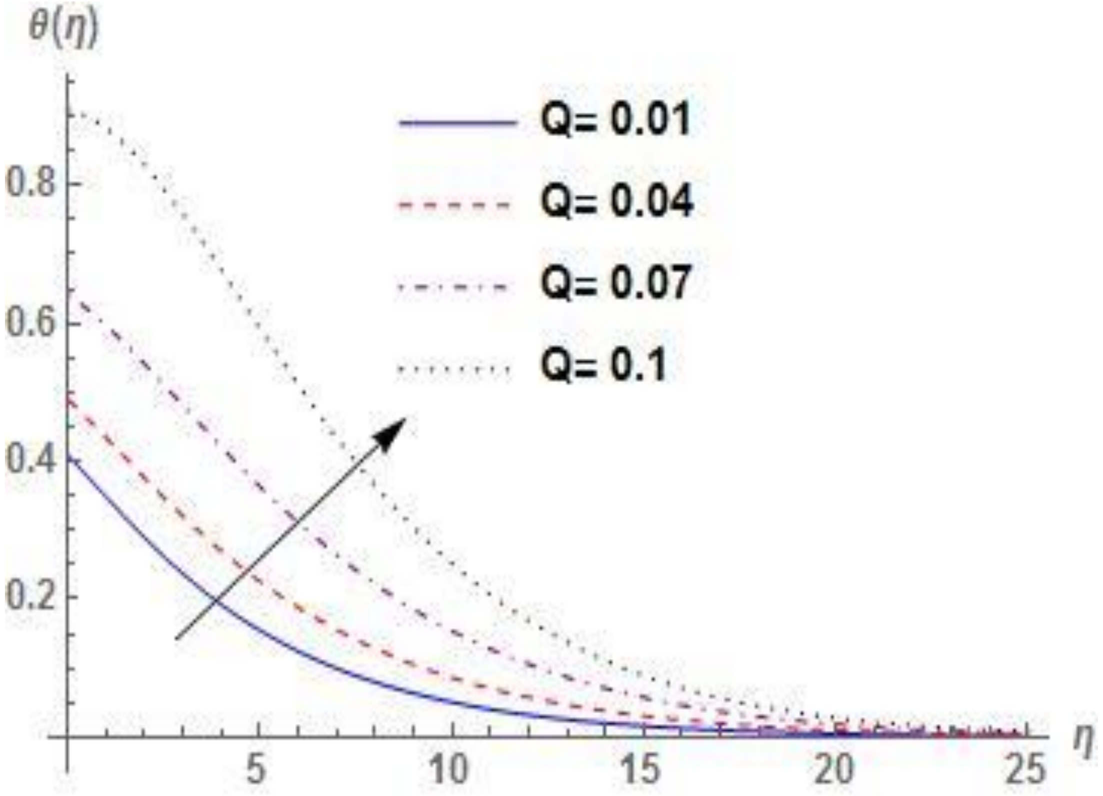

Fig. 7 significant of Q on Temperature $\theta(\eta)$

Conclusion

- ❖ large values of Ps suggest greater resistance to the motion of the fluid which reduces the motion of the fluid and lowers momentum boundary layer thickness
- ❖ the plate surface temperature is magnified on increase in heat generation and convective heat parameters, while the fluid temperature overshoot which consequently allow thermal effect to the quiescent fluid. Often used in Science and Technological field for drying of materials.
- ❖ The interaction of Magnetic parameter pioneer frictional heating within layer thereby results in an increase in fluid temperature

[1] Makinde OD. On MHD heat and mass transfer over a moving vertical plate with a convective surface boundary condition. Can J Chem Eng. 2010;88:983–990.

[2] Makinde OD. Similarity solution for natural convection from a moving vertical plate with internal heat generation and a convective boundary condition. Therm Sci. 2011;15:S137–S143

[3] Makinde, O.D. On MHD boundary layer flow and mass transfer past a vertical plate in a porous medium with constant heat flux. International Journal of Numerical Methods for Heat Fluid Flow, (2009)148 19(3/4),546554.

14] O.D. Makinde, Heat and mass transfer by MHD mixed convection stagnation point flow toward a vertical plate embedded in a highly porous medium with radiation and internal heat generation, Meccanica 47 (2012) 1173–1184.

[5] Hayat T, Mustafa M, and Pop I, "Heat and mass transfer for Soret and Dufour's effect on mixed convection boundary layer flow over a stretching vertical surface in a porous medium filled with a viscoelastic fluid," *Communications in Nonlinear Science and Numerical Simulation*, vol. 15(2010), no. 5, pp. 1183–1196.

[6] Hayat, A. Shafiq, M. Mustafa, A. Alsaedi, Boundary-Layer Flow of Walters B Fluid with Newtonian Heating, Z. Naturforsch, 70(5)a, 333341, 2015

[7] T. Hayat, Q. Sajid, A. Ahmed, A. Bashir, Magnetohydrodynamic (MHD) nonlinear convective ow of Walters-B nanouid over a nonlinear stretching sheet with variable thickness, International Journal of Heat and Mass Transfer, 110, 506514, 2017.

[8] Akinbo, B. J., Olajuwon, B. I., (2023) Interaction of radiation and chemical reaction on Walters' B fluid over a medium porosity of a vertical stretching surface. *Heat Transfer Journal*, 52(2): 1689-1709.

[9] Akinbo, B. J., Olajuwon, B. I., (2023) Impact of radiation and heat generation/absorption in a Walters' B fluid through a porous medium with thermal and thermo diffusion in the presence of chemical reaction. *International Journal of Modelling and Simulation*, 43(2): 87-100.

[10] Akinbo, B. J., Olajuwon, B. I., (2022) Viscous Dissipation Effect on Magnetohydrodynamics Fluid Flow Over an Exponential Surface with the Influence of Thermal Radiation and Thermal Diffusion. *European Journal of Computational Mechanics*, 31(5-6): 583-600

[11] Akinbo, B. J., Olajuwon, B. I., (2022) Stagnation-point flow of a Walters' B fluid towards a vertical stretching surface embedded in a porous medium with elastic-deformation and chemical reaction. *Journal of Heat and Mass Transfer Research*, 9: 27- 38.

[12] Akinbo, B. J., Olajuwon, B. I., (2021) Radiation and thermal-diffusion interaction on stagnation-point flow of Walters' B fluid toward a vertical stretching sheet. *International Communications in Heat and Mass Transfer*, 126: 105471.

[13] Akaje, T.W., Olajuwon, B. I., Raji, M. T., (2023) Effects of Homogenous-Heterogeneous reactions on stagnation point of aligned MHD Casson Nanofluid over a melting surface. Nigerian Journal of Technology, 42(1), pp. 2-11.

[14] Akaje, T.W., Olajuwon, B. I., Raji, M. T., (2023) Computational analysis of the heat and mass transfer in a Casson Nanofluid with a variable inclined magnetic field. Sigma Journal of Engineering and Natural Sciences, 41(3), pp. 1-12.

[15] Akaje, T.W., Taiwo, M. A., Olajuwon, B. I., Raji, M. T., Akinleye S. A., (2023) Double-Diffusive Nonlinear Buoyancy Force Significance on Free Convective Chemically Reacting Fluids Flow Past Vertical Riga Surface. Journal of Advanced Research in Fluid Mechanics and Thermal Sciences, 105(1), pp. 59-75.

[16] Akaje, T.W. and Olajuwon B.I. (2023) Dynamics of a Swimming Microorganism on Nanoparticle-Saturated Blood Flow under the Influence of Inclined Magnetic Field and Heat Source. *Computational Thermal Sciences* 15(3):1–22.

[17] Akaje, T.W. and Olajuwon B.I. (2022), The Effects of an Inclined Magnetic Field, Brownian motion, and Thermophoresis on the Flow of Electrically Conducting and Chemically Reacting Casson Nanofluids Using Soret-Dufour Mechanisms, Advances in Nanoparticles, 11, 55-71. https://doi.org/10.4236/anp.2022.112005.

Thank You